



The Effect of Helmet Mounted Display Field-of-View Configurations on Target Acquisition

By

**Victor Klymenko
Thomas H. Harding
Howard H. Beasley
John S. Martin**

UES, Incorporated

and

Clarence E. Rash

Aircrew Health and Performance Division

September 1999

19991005 032

DTIC QUALITY INSPECTED 4

Approved for public release, distribution unlimited.

**U.S. Army Aeromedical Research Laboratory
Fort Rucker, Alabama 36362-0577**

Notice

Qualified requesters

Qualified requesters may obtain copies from the Defense Technical Information Center (DTIC), Cameron Station, Alexandria, Virginia 22314. Orders will be expedited if placed through the librarian or other person designated to request documents from DTIC.

Change of address

Organizations receiving reports from the U.S. Army Aeromedical Research Laboratory on automatic mailing lists should confirm correct address when corresponding about laboratory reports.

Disposition

Destroy this document when it is no longer needed. Do not return it to the originator.

Disclaimer

The views, opinions, and/or findings contained in this report are those of the author(s) and should not be construed as an official Department of the Army position, policy, or decision, unless so designated by other official documentation. Citation of trade names in this report does not constitute an official Department of the Army endorsement or approval of the use of such commercial items.

Human use

Human subjects participated in these studies after giving their free and informed voluntary consent. Investigators adhered to AR 70-25 and USAMRMC Reg 70-25 on Use of Volunteers in Research.

REPORT DOCUMENTATION PAGE

Form Approved
OMB No. 0704-0188

1a. REPORT SECURITY CLASSIFICATION Unclassified		1b. RESTRICTIVE MARKINGS										
2a. SECURITY CLASSIFICATION AUTHORITY		3. DISTRIBUTION / AVAILABILITY OF REPORT Approved for public release, distribution unlimited										
2b. DECLASSIFICATION / DOWNGRADING SCHEDULE												
4. PERFORMING ORGANIZATION REPORT NUMBER(S) USAARL Report No. 99-19		5. MONITORING ORGANIZATION REPORT NUMBER(S)										
6a. NAME OF PERFORMING ORGANIZATION U.S. Army Aeromedical Research Laboratory	6b. OFFICE SYMBOL <i>(if applicable)</i> MCMR-UAD	7a. NAME OF MONITORING ORGANIZATION U.S. Army Medical Research and Materiel Command										
6c. ADDRESS (City, State, and ZIP Code) P.O. Box 620577 Fort Rucker, AL 36362-0577		7b. ADDRESS (City, State, and ZIP Code) Fort Detrick Frederick, MD 21702-5012										
8a. NAME OF FUNDING / SPONSORING ORGANIZATION	8b. OFFICE SYMBOL <i>(if applicable)</i>	9. PROCUREMENT INSTRUMENT IDENTIFICATION NUMBER										
8c. ADDRESS (City, State, and ZIP Code)		10. SOURCE OF FUNDING NUMBERS <table border="1" style="width: 100%; border-collapse: collapse; margin-top: 5px;"> <tr> <th style="width: 25%;">PROGRAM ELEMENT NO.</th> <th style="width: 25%;">PROJECT NO.</th> <th style="width: 25%;">TASK NO.</th> <th style="width: 25%;">WORK UNIT ACCESSION NO.</th> </tr> <tr> <td>62787A</td> <td>30162787A879</td> <td>XT</td> <td></td> </tr> </table>		PROGRAM ELEMENT NO.	PROJECT NO.	TASK NO.	WORK UNIT ACCESSION NO.	62787A	30162787A879	XT		
PROGRAM ELEMENT NO.	PROJECT NO.	TASK NO.	WORK UNIT ACCESSION NO.									
62787A	30162787A879	XT										
11. TITLE (Include Security Classification) The effect of helmet mounted display field-of-view configurations on target acquisition (U)												
12. PERSONAL AUTHOR(S) Victor Klymenko, Thomas H. Harding, Howard H. Beasley, John S. Martin, and Clarence Rash												
13a. TYPE OF REPORT Final	13b. TIME COVERED FROM TO	14. DATE OF REPORT (Year, Month, Day) 1999 September	15. PAGE COUNT 28									
16. SUPPLEMENTAL NOTATION												
17. COSATI CODES <table border="1" style="width: 100%; border-collapse: collapse; margin-top: 5px;"> <thead> <tr> <th style="width: 25%;">FIELD</th> <th style="width: 25%;">GROUP</th> <th style="width: 50%;">SUB-GROUP</th> </tr> </thead> <tbody> <tr> <td>23</td> <td>02</td> <td></td> </tr> <tr> <td>01</td> <td>03</td> <td>01</td> </tr> </tbody> </table>		FIELD	GROUP	SUB-GROUP	23	02		01	03	01	18. SUBJECT TERMS (Continue on reverse if necessary and identify by block number) helmet-mounted display (HMD) field-of-view (FOV), full binocular overlap, partial binocular overlap, convergent, divergent	
FIELD	GROUP	SUB-GROUP										
23	02											
01	03	01										
19. ABSTRACT (Continue on reverse if necessary and identify by block number) A helmet-mounted display with a partial binocular overlapping field-of-view (FOV) is slated for use with the Army's new RAH-66 Comanche helicopter in order to increase the available size of the FOV. There are three possible field-of-view configurations which are full overlap (FO), and the convergent and divergent partial overlap (CPO and DPO) configurations. We tested the effect of FOV configuration on visual performance by measuring response times and accuracy in a demanding target acquisition task. Fifteen aviators served as subjects. The results showed a trade-off in enlarging the FOV by partial overlap method. Response times were fastest and accuracy highest in the FO FOV. Response times were slowest and accuracy lowest in the DPO FOV and were intermediate in the CPO FOV. The performance decrements are most pronounced for lateral targets in the monocular regions of partial overlap FOVs.												
20. DISTRIBUTION / AVAILABILITY OF ABSTRACT <input checked="" type="checkbox"/> UNCLASSIFIED/UNLIMITED <input type="checkbox"/> SAME AS RPT. <input type="checkbox"/> DTIC USERS		21. ABSTRACT SECURITY CLASSIFICATION Unclassified										
22a. NAME OF RESPONSIBLE INDIVIDUAL Chief, Science Support Center		22b. TELEPHONE (Include Area Code) (334) 255-6907	22c. OFFICE SYMBOL MCMR-UAX-SI									

Acknowledgments

We thank Dr. William McLean and Dr. Gregory Francis for their critical review.

This work was completed under the U.S. Army Medical Research and Development Command Contract No. DAMD17-91-C-1081.

Table of contents

	<u>Page</u>
Introduction	1
Purpose of experiment	5
Method	6
Subjects	6
Equipment	6
Stimuli	8
Fields-of-view	9
Optical convergence, accommodation and fusion locks	9
Background clutter	11
Alphanumeric symbols	12
Design	14
Procedure	15
Data analysis	16
Results and discussion	16
Conclusions	24
References	26
Appendix	28

Table of contents (continued)

List of figures

	<u>Page</u>
1. In normal unaided vision the two monocular fields are partially overlapped producing a divergent FOV consisting of three regions, the central binocular overlap region and two lateral monocular regions.	2
2. Pilot's view of visual world in an HMD with a partially binocular overlapped FOV.	3
3. Perspective and schematic illustrations of the optical table configuration consisting of the monitor, eight mirrors, focusing lenses, and binoculars	7
4. Examples of the total FOV with targets and clutter	10
5. Examples of reduced FOV seen in FO FOVs	11
6. The two monocular fields on the monitor are each optically directed to an ocular of the binoculars for viewing by the subject	12
7. Mean response time to acquire target (FOV x Block).	17
8. Mean response time to acquire target (FOV x Position)	18
9. Mean number of misses before target acquisition (FOV x Position)	22
10. Mean percent of first scores (FOV x Position)	23

List of tables

1. Mean response time in seconds, collapsed over blocks, and planned comparisons	19
2. Mean percentage increase in response time, collapsed over blocks	19
3. Mean log of response times (in seconds), collapsed over blocks, and planned comparisons	21
4. Mean number of misses (out of a maximum of 8), collapsed over blocks	22
5. Mean percent of first scores, collapsed over blocks	23

Introduction

Monocular helmet-mounted displays (HMDs) currently are used in the Army's AH-64 Apache helicopter. A partial binocular overlap HMD is slated for use with the Army's new RAH-66 Comanche helicopter. The size of the binocular HMD's field-of-view (FOV) is the size of the visual world available to the Army helicopter pilot via an imaging sensor. The Comanche HMD presents the FOV in a partial binocular overlap configuration rather than a full binocular overlap configuration. In this latter configuration, the images presented to both eyes, the monocular fields, present identical views of the visual world where the FOV consists of a single binocular region. In the partial binocular overlap configuration, the FOV consists of a central binocular overlap region seen by both eyes, and two flanking monocular regions, each seen by one eye. What is the operational effectiveness of this new visual interface? First, we briefly describe the relevant differences between normal unaided vision and vision with a binocular HMD. Then, we cover our recent empirical findings on the sensory and perceptual effects of this type of display and how visual performance might be affected. Any deficits in performance need to be quantified before they are manifested on the battlefield. This study investigates how target acquisition is affected by implementing various configurations of the HMD's binocular display.

Normal unaided human vision consists of an overlapped divergent binocular FOV where the overall horizontal FOV is approximately 200 degrees of visual angle (when viewed straight ahead), with each eye's monocular field around 120 degrees of visual angle. The two partially overlapping monocular fields produce an FOV consisting of three regions. The central binocular region, which both eyes can see, is approximately 120 degrees, and the two lateral monocular regions, seen exclusively by each eye, are each approximately 40 degrees. The FOV is divergent because the right eye sees the monocular region to the right of the overlap region, and the left eye sees the monocular region to the left of the overlap region (Figures 1 and 2).

Current technology limits the size of the monocular fields an HMD can present to each eye due to the weight and size of the HMD oculars and the need for adequate eye clearance. Small FOVs can be detrimental to the visual tasks required of military pilots (Kenyon and Kneller, 1993; Osgood and Wells, 1991; Wells, Venturino, and Osgood, 1989; Wolpert, 1990). Relative to full overlap (FO), the horizontal FOV of HMDs can be increased, without increasing the size of the monocular fields, by partially overlapping the HMD's FOV (Melzer and Moffitt, 1989, 1991). The partial overlap (PO) configuration can be either divergent or convergent. The HMD's monocular fields can be overlapped in the divergent configuration as in normal vision. The resulting visual regions will be smaller than for normal vision because the HMD's monocular fields are smaller than each eye's normal view. Alternatively, the HMD can be overlapped in the convergent partial overlap (CPO) configuration, where contrary to the divergent partial overlap (DPO) configuration, the right eye instead will see the monocular region to the left of the binocular overlap region, and the left eye will see the monocular region to the right. If the monocular regions are in the FO configuration, the FOV will be one binocular region limited to the size of a monocular field (Figure 2).

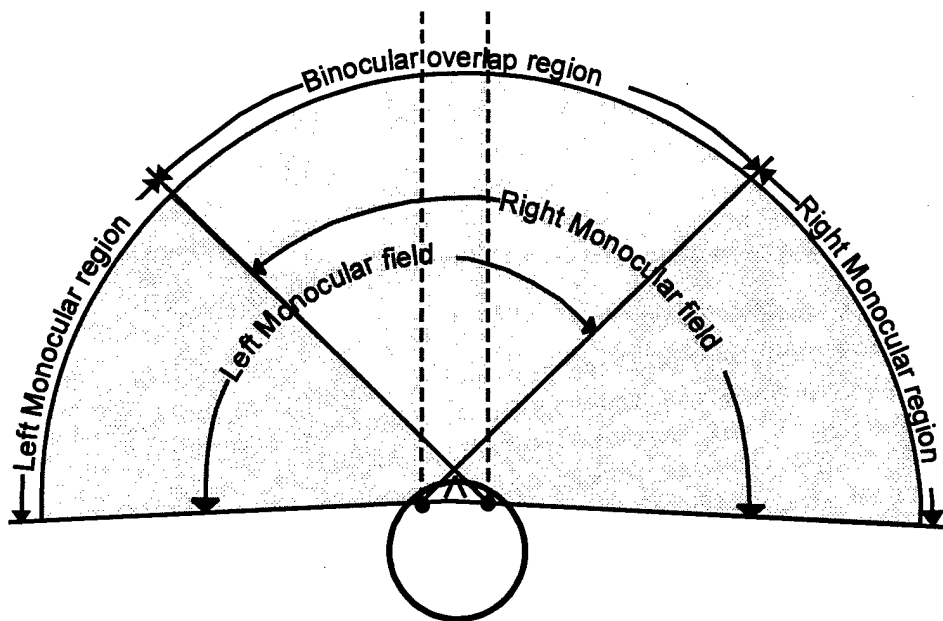


Figure 1. In normal unaided vision the two monocular fields are partially overlapped producing a divergent FOV consisting of three regions, the central binocular overlap region and two lateral monocular regions.

The PO method was designed to increase the limited FOV available in the HMD without incurring unacceptable increases in the size and weight of the HMD or losses in central resolution. However, increasing the FOV by this method has been a concern (Alam et al., 1992; Edgar et al., 1991; Kruk and Longridge, 1984; Landau, 1990; Moffitt, 1989; Moffitt, 1991; and Moffitt and Melzer, 1991). One detrimental consequence of the partial binocular overlap display configuration is the perceptual effect known as luning (Figure 2), which is a subjective darkening of the monocular regions near the binocular overlap border (Moffitt, 1989; Klymenko et al., 1994b). Luning can lower the visibility of stimuli as well as distract the pilot using the HMD. Fragmentation can also occur in partial overlap displays. This refers to the segmented phenomenal appearance of the display as three distinct regions instead of the perceptually unitary FOV normally seen (Klymenko et al., 1994a). The detrimental visual effects of luning and visual fragmentation tend to be greater in divergent than in convergent displays (Klymenko et al., 1994a,b). The most likely reason for this is as follows. The partially overlapped FOV of the HMD, which is smaller than the FOV in normal vision, results in the display's central binocular

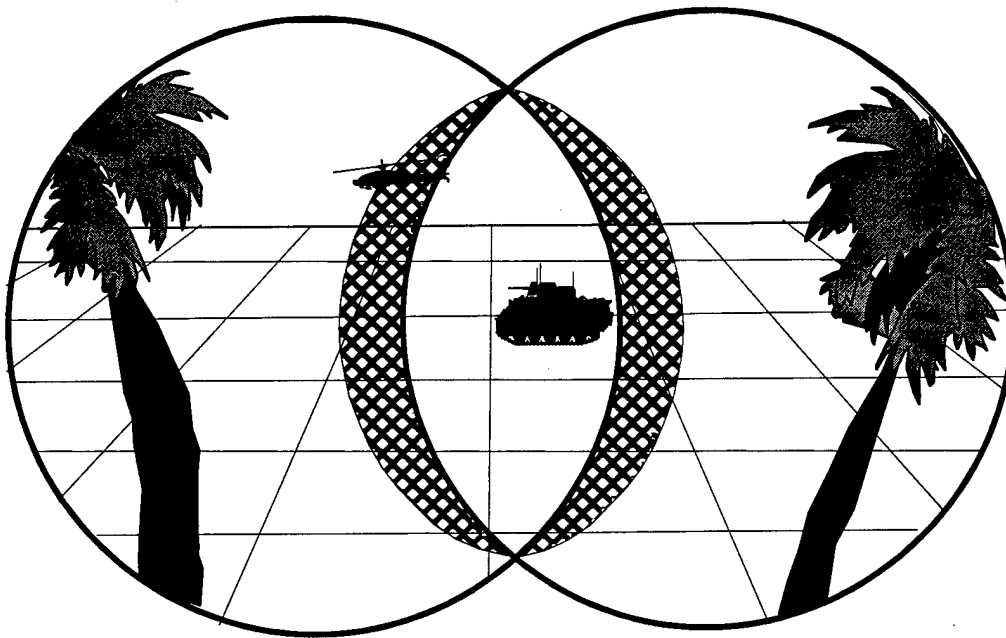


Figure 2. Pilot's view of visual world in an HMD with a partially binocular overlapped FOV. Each eye sees a circular monocular field against a black background. The real world image to each eye matches in the binocular region, but in the monocular regions, the real world image of each eye is matched to the black background of the other eye leading to visual effects such as binocular combination and binocular rivalry. Luning, the temporally varying subjective darkening near binocular overlap borders, can result. Also, fragmentation of the FOV into three phenomenally distinct regions and reduced target visibility in monocular regions can occur.

region and two flanking monocular regions falling in a visual area that is normally completely binocular. Visual processes such as binocular rivalry and dichoptic competition become visually pronounced and are experienced as luning and fragmentation in the FOV. (See extensive discussions in Klymenko et al., 1994a,b,c.) Also, there is an effect on the visibility of targets in the monocular regions of partially overlapped FOVs.

The visibility of targets, and the visual world in general, seen in the HMD's FOV is of paramount importance to military aviators. In a target detection task, where the contrast needed to see a target was compared across display configurations, Moffitt (1989) found no significant

effects of partially overlapping the displays. Target visibility, as measured by the degree of contrast needed to simply detect the presence of a target in a blank field, was unaffected by the method of overlap. Klymenko et al.(1994c), however, did find a difference in target visibility as measured by the degree of contrast needed to determine the orientation of a target. The results showed that targets were most visible in the FO FOV display, least visible in the DPO FOV, and intermediately visible in the CPO FOV. Other display factors were also found to effect target visibility. Targets in the binocular region were, as expected, more visible than targets in the monocular region. Also, targets in the monocular region adjacent to the binocular overlap border were less visible than more displaced targets. The target visibility effects were relatively small in terms of contrast, but were clear cut and systematic.

The reason for the reduced target visibility in PO FOVs is the dichoptic competition between the two eyes due to conflicting visual information. This includes a general visual system effect of binocular rivalry (and alternating monocular dominance) between the two eyes, and a specific stimulus effect due to the binocular overlap border in the display. For more extended discussions see Klymenko et al. (1994a,b,c).

Klymenko et al. (1994c) used the threshold contrast for orientation determination as a measure of target visibility. Are these reduced target visibility effects likely to affect general visual performance? The increase in target thresholds in the DPO FOV display compared to the CPO FOV and the increase in both of these compared to the FO FOV were small and might arguably be a negligible effect. The contrast thresholds differed usually by only a few percent in modulation contrast (Klymenko et al., 1994c). Those findings were from a psychophysical study concerned with the effect on the visual system response and not with the effect on visual performance under realistic operational conditions. Therefore, the viewing procedure had been optimized in a number of ways. Subjects always knew the location of the target and fixated it during the contrast threshold setting procedure. They had unlimited time to view each target and to set the threshold, and the target remained in one location throughout an experimental session. Also, there were no additional demands on the subject; that is, the mental workload, the drain on attentional capacity, was nil. What would happen to the small differences in human responses to different FOV configurations if these factors were less optimal? Will the small differences disappear or be magnified under nonoptimal, more operationally realistic, viewing conditions?

It is possible that the optimization of viewing conditions for contrast threshold in Klymenko et al. (1994c) may have alleviated the deleterious effects of partial binocular overlap displays. If so, these effects may be more serious than the small thresholds seem to imply. For example, the lack of time constraints in our previous experiment may have reduced the effect of binocular rivalry because the subject had time to voluntarily shift attention between the two eyes, or to simply wait for an optimal phase in the temporal progression of binocular rivalry. Also, direct fixation and knowledge of location may help lower contrast threshold by reducing uncertainty. In short, the differential effects we found may have been minimized by the optimal viewing conditions by pushing all the results towards a common floor (the lowest possible thresholds). Normal viewing in the real world is seldom so optimal, especially in a military

aviation environment. Therefore, the effect of the HMD display configuration on visual performance under realistic viewing conditions remains an open question.

In short, previously, we have found differences in human vision due to the different display configurations. Those results showed less visual impairment in FO FOVs than in PO FOVs, and between the PO FOVs, there was less impairment under the CPO FOV than under DPO FOV. How important are these psychophysical differences in practical terms? The current study was designed to gain more understanding of the real world impact of these HMD designs on general visual performance by using a target acquisition task under the more realistic psychological constraints experienced in aviation. This included time pressure, uncertainty of target location and orientation, multiple possible targets and nontargets, nonstationary targets, a randomly cluttered background, and a requirement for scanning eye movements across the FOV. This was a higher mental workload task demanding more attentional capacity. Would this difficult task alleviate or exacerbate the differences between the display configurations? In other words, would the small, yet systematic, perceptual differences induced by the different FOV configurations be mirrored in visual performance under more realistic and demanding viewing conditions, or will they disappear? Aviation is an attention demanding (high mental workload) environment with a high rate of visual information throughput where visual inspection time is limited. Often the eyes need to continually scan an FOV with a moving visual scene and moving targets. This is a stimulus environment that often taxes the visual performance of the human perceiver, who has been described as a limited capacity processor of visual information. Under operational conditions, human performance may be compromised by the PO FOV design. The performance decrements with these HMDs may become critical in attention demanding environments such as military aviation. This study assesses the effects of these FOV configurations on visual performance under more demanding viewing conditions.

Purpose of experiment

The current investigation was designed to determine how display configurations affect visual performance in a target acquisition task under demanding viewing conditions. The purpose was to measure the effect of partial binocular overlap on visual performance. The viewing conditions are designed to simulate the high visual information throughput an aviator might experience under operational conditions. Performance in three different FOV configurations was measured by response time (RT) and error rate. The three configurations were the FO, the CPO, and the DPO FOV. The task required subjects to visually scan for and identify the target's position in a randomly cluttered FOV as quickly as possible while minimizing errors. The target could be in any one of nine locations and could be any member of a subset of a larger total set of similar objects, all of which were visually degraded. Monocular field size was controlled across display configurations, meaning that the same sized monocular fields were used in the FO and the two PO FOVs.

Except for orientation contrast threshold and perception of luning and fragmentation (Klymenko et al., 1994a,b,c), we do not currently know which factors, and their relative

importance, might be influenced by the type of FOV configuration. We therefore implemented a number of factors likely to reveal differences. These included the physical characteristics of the targets, and the target positions. For dichoptic stimulation, figures with sharp edges and sharp temporal onsets and offsets tend to be better dichoptic competitors, and so more visible in the fused binocular percept than figures with smooth edges and smooth temporal offsets and onsets. Therefore, the targets used in the experiment were spatially blurred and presented with smooth temporal onsets and offsets. In PO displays, targets are likely to be least visible in the monocular regions adjacent to the binocular borders (Kaufman, 1963,1964; Klymenko et al., 1994c); therefore, positions located there were included among the scanned positions.

In this preliminary study, a number of factors were psychophysically designed to induce differences between FOV configurations in order to determine the practical relevance of the FOV configuration in terms of visual performance. The displays and task were unique to the experiment, so prior experience with particular HMDs and symbology would not be a factor.

Method

Subjects

Fifteen Army aviators, 13 males and 2 females, voluntarily took part in the experiment. This population had passed class II flight physical vision tests. All had 20/20 unaided or better Snellen acuity. Mean age was 31.8 (SD = 6.3), ranging from 24 to 42.

Equipment

The equipment consisted of three major components: A Hewlett-Packard HP-98731 Turbo-SRX computer graphics workstation used to generate the visual stimuli, a custom optical table configuration used to optically direct the visual stimuli from the workstation monitor to a pair of viewing binoculars, and a subject booth. The booth was a light-proof enclosure behind the binoculars where the subject viewed the stimuli via the binoculars and responded via an HP response keypad, the "buttonbox."

The HP-98731 Turbo-SRX computer graphics workstation consisted of a 19-inch color Trinitron monitor (1280 x 1024 pixels) for presenting visual stimuli and a computer for generating the stimuli, recording the responses, and analyzing the data. Connected to the workstation were the experimenter's terminal to allow the experimenter to run the experimental programs and monitor the progress of each experimental session, and the buttonbox to allow the subject to respond to the visual stimulus presentations.

The optical table configuration consisted of a 4-foot x 6-foot optical table, with the workstation monitor mounted at one wide end of the table, and eight front-surfaced mirrors mounted on the table to direct the visual image--the optical train--to a pair of viewing binoculars

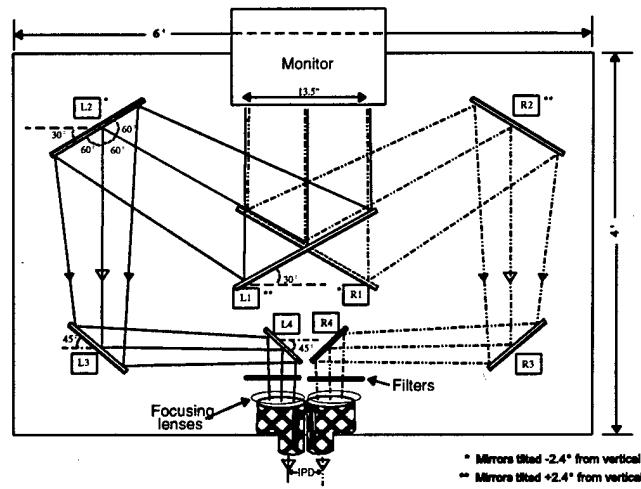
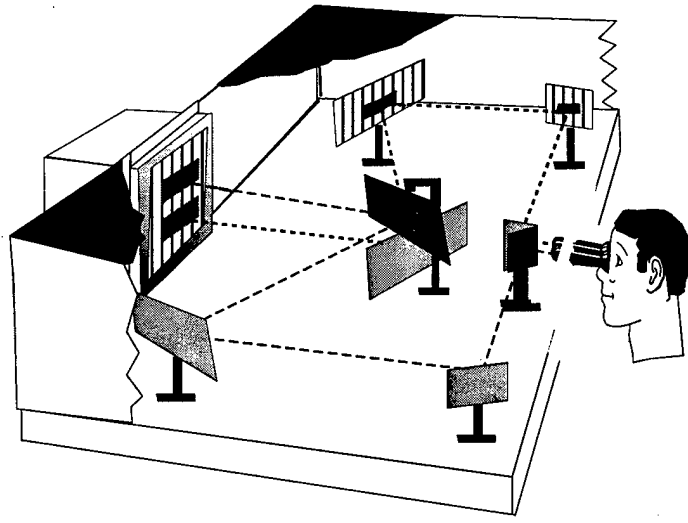


Figure 3. Perspective and schematic illustrations of the optical table configuration consisting of the monitor, eight mirrors, focusing lenses, and binoculars. Top image of monitor is directed to left eye, and bottom image is directed to right eye.

mounted on the other wide end of the table (Figure 3). The mirrors allowed the independent presentation of two channels, one to each ocular of the binoculars, from the same monitor. Through the binoculars, the image on the top half of the monitor was seen by the left eye and the image on the bottom half of the monitor was seen by the right eye. The 7x50 binoculars were mounted within a fixture which allowed the interpupillary distance (IPD) to be adjusted for each subject. Affixed on the front of the binoculars were auxiliary focusing lenses to focus the magnified image for the optical train viewing distance. A light baffle in front of the monitor between the two optical paths was positioned to prevent cross talk between the two image channels. The two mirrors, L4 and R4 in Figure 3, mounted directly in front of the binoculars, were movable to allow adjustments corresponding to the IPD settings of the binoculars.

The images seen through each ocular of the binoculars were 50 degrees of visual angle corresponding to 1280 pixels. The spatial resolution of the display was 25.6 pixels per degree of visual angle as seen through the binoculars. The temporal resolution, or frame rate of the monitor, was 60 Hz noninterlaced. The luminance resolution was 256 driving levels. The driving level to luminance conversions are given below. The 7x50 binoculars have a vertex distance of 27 mm and an exit pupil diameter of 7.14 mm. The subject, within reach of the buttonbox, was seated at a chin rest in the light-proof subject booth in front of the binoculars. Except for the stimuli viewed through the binoculars, the subject was in darkness.

Stimuli

The stimuli consisted of a series of computer generated displays, where each display contained one of three FOV configurations. Each FOV contained a 3 by 3 array of blurred and flickering alphanumeric symbols, eight of which were random letters and one a random numerical digit, which was the target. Also, described below, each FOV contained 6 small crosses for fusion locks and 30 random ellipses for background clutter. Stimulus details are given below and examples are shown in Figures 4-6.

Stimulus luminance values, in terms of computer driving levels, ranged from 0 (black, 0.01 fL) to 255 (white, 31.67 fL), with intermediate values of 64 (dark grey, 1.33 fL), 128 (neutral grey, 6.65 fL) and 192 driving levels, (light grey, 16.81 fL). Half of the ellipses were light grey and half were dark grey, and the FOV background was neutral grey. The area outside the FOV was black, as were the fusion locks and the alphanumeric symbols (before blurring). Before display, the symbols were processed by blurring. Blurring causes the luminance of a symbol's pixels (and neighboring pixels) to vary in a complex way with different pixels taking on different values. The values were between the symbol's original pre-blurred value (black) and the values of the symbol's local surround, which could be light, dark and/or neutral grey. The displayed driving levels were computed from the preblurred driving levels, and then the blurred symbol was temporally modulated for display as described below.

Fields-of-view

The total FOV was a rectangular area, 32.8 degrees of visual angle horizontal (840 pixels) by 10 degrees of visual angle vertical (256 pixels) (Figure 4). Subjects saw parts of the total FOV by the monocular fields presented to each eye. The monocular fields were each 23.4 horizontal degrees of visual angle, 600 pixels, by the full vertical extent. The FOV display configurations differed in the portions of the total FOV presented to the monocular fields of each eye. In the FO FOV configuration, each eye's monocular field displayed the same central portion of the total FOV, so that the FOV seen by the subject was binocular. In the DPO configuration, the right eye's monocular region was the rightmost 9.4 degrees of the potential FOV, and the left eye's monocular region was the leftmost 9.4 degrees of the potential FOV. Conversely, in the CPO configuration the right eye's monocular region was the leftmost 9.4 degrees of the total FOV, and the left eye's monocular region was the rightmost 9.4 degrees of the FOV (Figure 5).

In both PO conditions, the FOV seen by the subject was the full 32.8 degrees of the total FOV. This FOV consisted of a 14.1 degree central binocular region, and two flanking 9.4 degree monocular regions, with each eye seeing the monocular regions as described. In the FO condition, the FOV seen by the subject was the central 23.4 degree portion of the total FOV. In the FO condition, the binocular region was larger than in the PO conditions, while in the PO conditions an enlarged FOV is seen with a smaller binocular region.

These FOVs were presented by drawing each eye's monocular field separately on the top and bottom halves of the monitor (Figure 6), and directing the images to each eye's view through the binoculars via the optical table configuration (Figure 3).

Optical convergence, accommodation and fusion locks

Optical convergence and accommodation were both set for 2 meters. Optical convergence here refers to the angle between the optical axes of the eyes and should not be confused with the CO FOV configuration. Since the centers of both the right eye and the left eye images were focused to 2 meters (-0.50 diopter) through the binoculars, the right and left images also were positioned so that the eyes converged to 2 meters. This was done by shifting each eye's image on the monitor 0.86 degree of visual angle (22 pixels) in the nasal direction.

Subjects require similar stimuli common to both eyes to prevent disjunctive eye movements in order to binocularly fuse images properly and to avoid image slippage, which leads to the binocular overlap of inappropriate regions of the two monocular images. To ensure binocular locking of the appropriate areas of the monocular fields, and to provide a way to monitor binocular fusion, fusion locks were present in each display. These were six crosses, three in the upper center of the total FOV and three in the lower center. Subjects were told that they should see three crosses above and below the center of each display. If they saw more, then the images were not properly fused, and they should tell the experimenter. This did not occur. With the background clutter described below, there were ample binocular stimuli to prevent slippage.

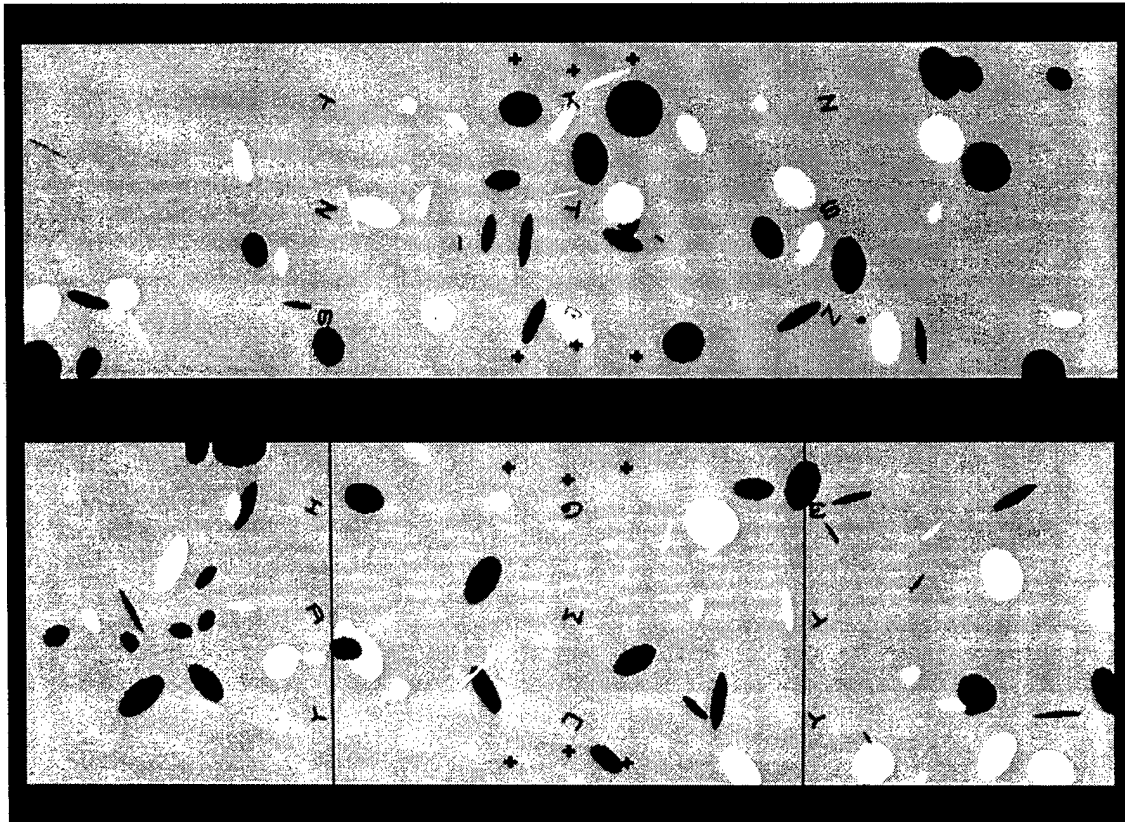


Figure 4. Examples of the total FOV with targets and clutter. The top shows the total FOV with nine alphanumeric symbols, six fusion locks (crosses), and random clutter (ellipses). Target is the "6" in the left bottom position. The horizontal extent is 32.8 degrees of visual angle, and the vertical extent is 10 degrees of visual angle. In the PO FOV configurations, this is presented to the subject via two monocular fields, each 23.4 degrees of visual angle in horizontal extent.

The bottom shows the location of the monocular field borders, which in the FOV become binocular borders, separating the three regions of the PO FOV. The right monocular field contains the center and right regions, and the left monocular field contains the center and left regions. In a DPO FOV, the right monocular field is presented to the right eye and the left field to the left eye, whereas in the CPO FOV, this is reversed. In FO FOVs, a smaller portion of the total FOV is seen as shown in Figure 5.

Note: Grey levels in Figures 4-6 are not faithfully reproduced by photography.

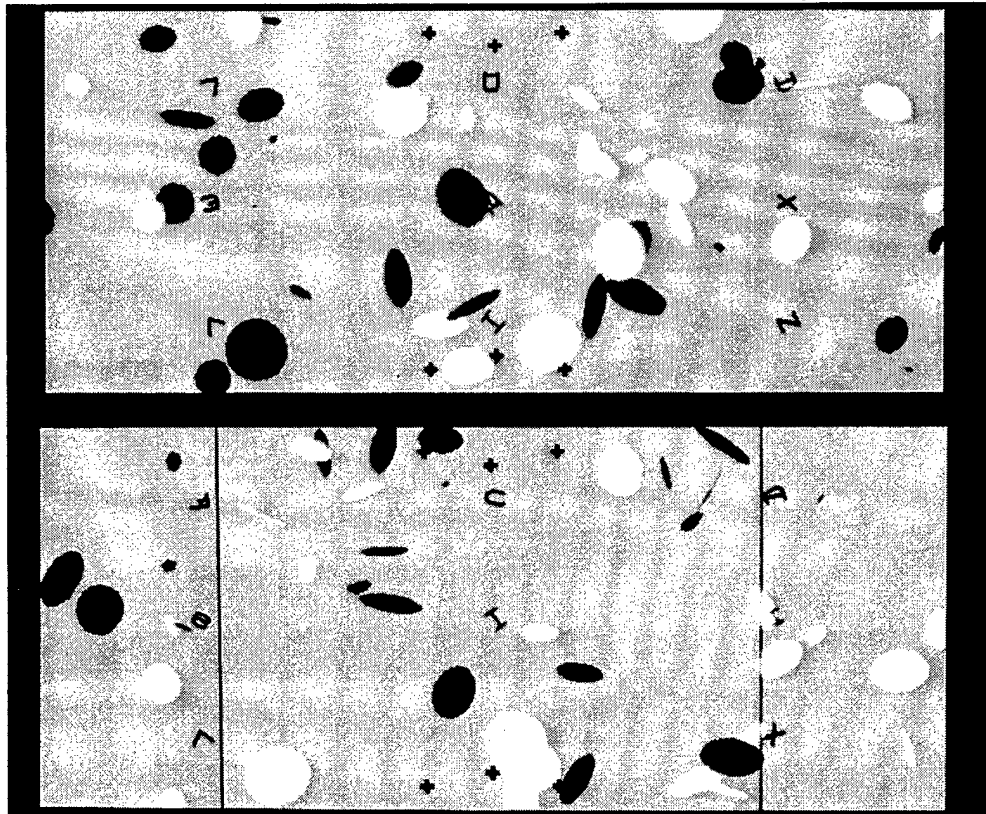


Figure 5. Examples of reduced FOV seen in FO FOVs. The top shows the FO FOV, where both monocular fields present the same center region (23.4 degrees of visual angle in the horizontal extent) to each eye. The bottom shows how much the binocular portion of the FOV is shrunk in the PO FOVs. Figure 4 shows how the FOV is enlarged by PO.

Each shaft of the crosses was 8 pixels long by 2 pixels wide. Center crosses were 25 pixels from the top and bottom of the FOV and flanking crosses were located 44 pixels to the right and left of the center and 16 pixels from the top and bottom of the FOV.

Background clutter

For clutter, each display contained 30 ellipses, randomly oriented, randomly sized, and randomly positioned. The center of each ellipse could, with equal probability, be located on any pixel within the total FOV. The orientation of each ellipse could, with equal probability, be anywhere from 0 to 180 degrees. Ellipse size was randomized by sizing each of the two axes of each ellipse with equal probability anywhere from 1 to 44 pixels in length. Of course, only the

portion of each ellipse falling in the monocular fields were displayed in the FOV. Ellipses were alternatively light and dark grey, with later ellipses drawn over former ellipses and the alphanumeric symbols drawn last.

Alphanumeric symbols

In each display, one of nine alphanumeric symbols was the target number and the remaining eight were nontarget letters. Alphanumeric symbols were all in "stick figure" font, or font number 1, predefined in the Hewlet-Packard Starbase computer graphics language. Letters were all capitals, and all alphanumeric symbols were defined within a 16 by 16 pixel symbol square (1.6 by 1.6 degrees of visual angle). Alphanumerics were initially 0 driving levels, the background of the FOV was 128, and the light and dark ellipses were 192 and 64 driving levels, respectively. Before display, each symbol was preprocessed by rotating and blurring. The orientation of each symbol was randomized by rotating the symbol randomly from 0 to 360 degrees.

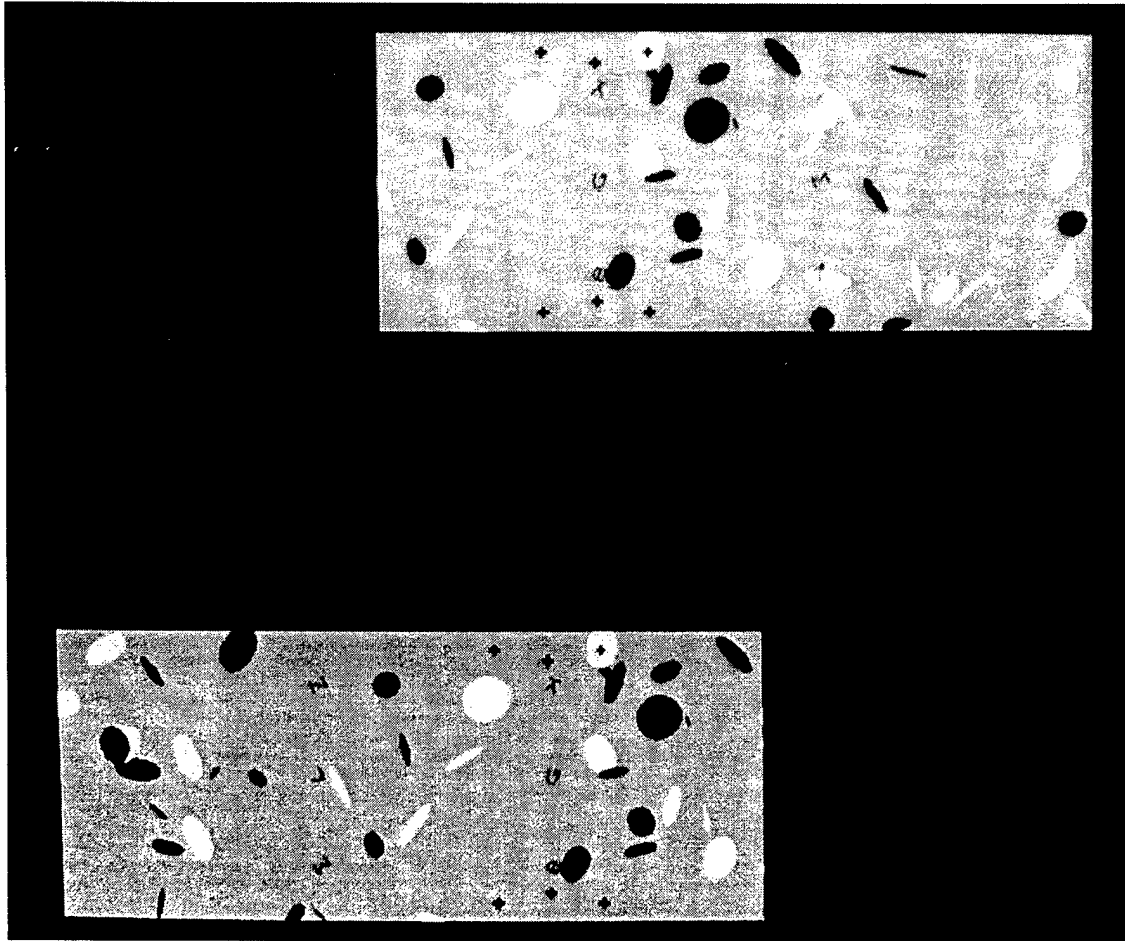


Figure 6. The two monocular fields on the monitor are each optically directed to an ocular of the binoculars for viewing by the subject.

Spatial blurring of the symbol was implemented as follows. The original 16 by 16 symbol square consisted of symbol pixels and non-symbol pixels. The symbol pixels and adjacent non-symbol pixels were defined as the blur zone. This blur zone included any symbol pixel, that is a pixel that contained part of the alphanumeric symbol, and any non-symbol pixel that was adjacent to a symbol pixel, adjacency defined as the eight contact pixels. The pixels in the blur zone were then filtered by a 3 by 3 Gaussian kernel. This means, that for each blur zone pixel, the old driving level was replaced by a new driving level, which was the weighed average of the old value and the driving levels of the eight pixels around it. The kernel weights were as follows where the central 12 represents the weight of the old driving level:

$$\begin{array}{ccc} 1 & 4 & 1 \\ 4 & 12 & 4 \\ 1 & 4 & 1 \end{array}$$

Therefore, symbols were blurred into the background, which included the FOV background and any ellipse adjacent to the symbol. The new blurred symbol thus contained more pixels with smoother transitions between symbol and background.

Temporal modulation was implemented by passing the blurred symbol through a series of lookup table functions, one function for each frame of the temporal sequence. In the lookup table function, each original input driving level in the blurred symbol was changed to an output displayed driving level. Cycling through the set of functions caused the original stimulus's luminance to change smoothly from identity at one extreme, where the original blurred symbol was displayed, to invisibility at the other extreme, where all the pixels were equal to the background of the FOV (128). This was done by the following lookup table equation:

$$y = x * \tan(\text{angle}) - (128 * \tan(\text{angle})) + 128,$$

where x = input pixel driving level; y = output pixel driving level; and angle = 0 to 45 degrees in steps of 2.5 degrees.

Angle represents the slope of the input-output lookup table function which was changed for each frame of the temporal modulation sequence. At one extreme, the angle equaled 45 degrees, causing all displayed driving levels (y) to equal all original input driving levels (x), that is, the original blurred image was displayed. At the other extreme, where the angle equaled 0 degrees, all output driving levels (y) equaled 128, where the entire blurred symbol was the same driving level as the background of the FOV and therefore invisible with respect to it. Between 0 and 45 degrees, each of the symbol's driving levels was intermediate between 128 and the original value.

Eighteen frames were created by incrementing the angle from 0 to 45 degrees in steps of 2.5 degrees. The frames were displayed in the sequence 1 - 19, 18 - 2 for a full modulation cycle of 36 frames, with cycles repeating until the subject responded correctly. Frames were presented

at the rate of 30 per second, with a frame duration of 33.3 msec. With 36 frames in a full modulation cycle, the flicker rate was 0.83 cycles per second, or 1.2 seconds per cycle. The flicker cycle smoothly varied the symbol contrast between maximum visibility, the original blurred symbol, and invisibility (i.e., invisible with respect to the background of the FOV). All symbols slowly faded into and emerged from the background by appearing and disappearing. When the angle was 0, a symbol may have still been visible if it was on or near an ellipse, because the symbol's driving level of 128 was distinguishable from the ellipse driving level of 64 or 192. All nine flickering symbols were in phase. Stimulus onset started at invisible.

The nine symbol positions were in three columns and three rows. Defined from the center of the symbol, one column was 2 pixels to the right of the FOV center. The left column was 195 pixels to the left, 7.5 degrees of visual angle to the left of center. The right column was 189 pixels to the right of center, 7.4 degrees of visual angle to the right of center. When in the PO FOVs, the left column was two pixels away from the edge of the monocular field border, and the right column was adjacent to the monocular field border. This is in terms of the 22 x 22 pixel square of the potential occupied region of each letter after blurring and rotation (Figures 4-6). One row was centered in the middle of the FOV, and the other two were 80 pixels, or 3.1 degrees, above and below the middle row (center to center). Column positions are referred to as Right (R), Center (C), and Left (L); and row positions are referred to as top (t), middle (m), and bottom (b), generating the nine designations: Rt, Rm, Rb, Ct, Cm, Cb, Lt, Lm, Lb. For the DPO and CPO FOVs, the right and left columns of symbols outside the overlap border were monocular stimuli, as opposed to the center column of symbols which were binocular. Under the FO FOV configuration all the symbols were binocular.

Design

Each trial consisted of a unique display to which the subject responded. In the experiment, there were 216 trials presented in 6 blocks, where each block contained 3 FOV configurations, FO, DPO, and CPO, presented in random order. For each FOV configuration, there were 12 trials. Unknown to the subject, the first 3 of these 12 were considered practice to allow the subject to acclimate to the FOV, and the data were not recorded. From the subject's point of view, which of the nine positions the target occupied, and which number symbol was used for the target, was random on each trial. In fact, the position of the target was random with replacement for the first three trials in each FOV, and random without replacement for the final nine trials for which the data were recorded. Across displays, the number that was the target was randomized with replacement from the following seven numbers, 2, 3, 4, 5, 6, 8, 9. Within displays, and across displays, each of the eight nontarget letters was randomized with replacement from a set of 23 letters (alphabet minus the letters O, Q and L). The experiment was a 6 (block) x 3 (FOV configuration) x 9 (position) design.

Procedure

The subjects' interpupillary distance was measured and the equipment adjusted accordingly. The mean interpupillary distance for the 15 subjects was 61.3 (SD = 1.8). Subjects were given instructions and assurances of anonymity, and signed the consent form. Then subjects adjusted the chin rest, keypad, and height of the seat for comfortable viewing of the display through the binoculars.

To ensure there was no visual clipping of the FOV, or vignetting, for the area which would contain the experimental stimuli, a binocular display containing three widely spaced circles was shown. It contained the same optical convergence as the stimulus displays. The three circles were superimposed over a purple background with a white grid. There was a black circle in the center of the display, a blue circle to the right of center, and a yellow circle to the left of center. The black circle was 24 pixels in diameter and the outer two circles were 34 pixels in diameter. The outer edges of the outer circles were 668 pixels (26.1 degrees) distance from each other. The subjects were asked if they could see, without moving their head position, the entire yellow circle, the entire blue circle, and the grid surrounding each circle clearly and without vignetting when they visually scanned across the display.

In the experiment, subjects viewed a series of stimulus displays, each with nine alphanumeric symbols in nine standard positions. One symbol was always a number, and the remaining eight were always letters. The subjects were told the following: There would be nine symbols in each display, one of which was the target number. The symbols would be blurred, randomly oriented and flickered. Their task for each display was to identify the position of the number as quickly as possible by hitting the appropriate key on the keypad, and to avoid misses; that is, avoid hitting non-targets. The nine keys in the keypad were configured in a 3 by 3 array corresponding to the nine potential positions of the target. To induce the need for rapid response, as well as the need to maintain accuracy, subjects were told to imagine that the target number symbol was the enemy which would shoot them if they did not shoot it first, and the nontarget letter symbols were friendlies. The computer calculated the percentage of targets, including the practice trials, over each block that were acquired on the first try without misses. At the end of every block, this percentage appeared on the screen to motivate the subject to maintain accuracy and avoid random guessing.

To accomplish the task, the subject needed to scan the entire display, compensating for the symbol rotations and blurring, and catching the symbols when they were visible and quickly deciding which symbol in the display was the number. The subjects were told to respond as quickly as possible while maintaining accuracy. For every change of FOV, the letters "OK" appeared in the center of the first display of the new FOV without the targets. Subjects were told that for these displays they could pause if they wanted, and then initiate the next series by hitting a start key.

Once the series of displays started, for each display, the image would remain on until the target was hit. If an error was made, a transient asterisk appeared in the location of the letter to indicate that it was not the target. When the key was released, the letter returned. When the target number was identified by hitting the correct key, the screen went blank and 2.5 seconds later a new FOV appeared.

To familiarize themselves with the task and targets, the subjects first ran one block with a practice program, where each of the three FOVs contained six displays, with random target position without replacement, and no clutter ellipses in the FOV. Then they practiced with the same program with the clutter ellipses for from one to three FOVs, as determined by when they felt comfortable with the task. Then four minutes later, they ran the experiment.

Data analysis

The data were analyzed in a three-way repeated measures analysis of variance (ANOVA) where the 162 treatments consisted of 6 Blocks times 3 FOV configurations times 9 Positions. Four types of data were collected. These included RT, the time to indicate the correct target; and logRT, where the log of each of the response times served as the data. The log of response time is typically used as a check in reaction time and response time data analysis to remove the undue influence of outliers. As a further check on the data, the number of misses before acquiring the correct target was recorded for each trial. The percent of first scores, that is the percent of no-miss target acquisitions, was also recorded. The number of misses meant the number of wrongly acquired targets on each trial; which, as there were nine symbols, could be a maximum of eight for each trial, and a minimum of zero if the first target acquired was the correct one. The percent of first scores was calculated as follows: A condition was scored as one for each trial in which the target was hit on the first guess, and zero if the first guess was incorrect, that is a miss. The RT (and logRT) measures performance speed, and the number of misses and the percent of first scores measure performance accuracy.

Results and discussion

For RTs, the three-way Blocks x FOV x Position interaction was not significant, $F(80,1120) = 1.02$, $p = .43$. The two-way Block x FOV interaction was not significant, $F(10,140) = 0.32$, $p = .97$ (as shown by the rough parallelism between FOV configurations in Figure 7), and the two-way Block x Position interaction was not significant, $F(40,560) = 1.38$, $p = .06$. The two-way FOV x Position interaction was significant, $F(16,224) = 4.11$, $p = .000001$ (indicated by the overlapping FOV lines in Figure 8). The focus of this study, the effect of FOV on RT, is examined below for each position.

For RTs, there was no interaction between the Blocks factor and either, or both, of the other two factors. The main effect of Blocks on RT was significant, $F(5,70) = 6.55$, $p = .000047$. There is a general decline in RT over blocks which can be seen in Figure 7, where each of the

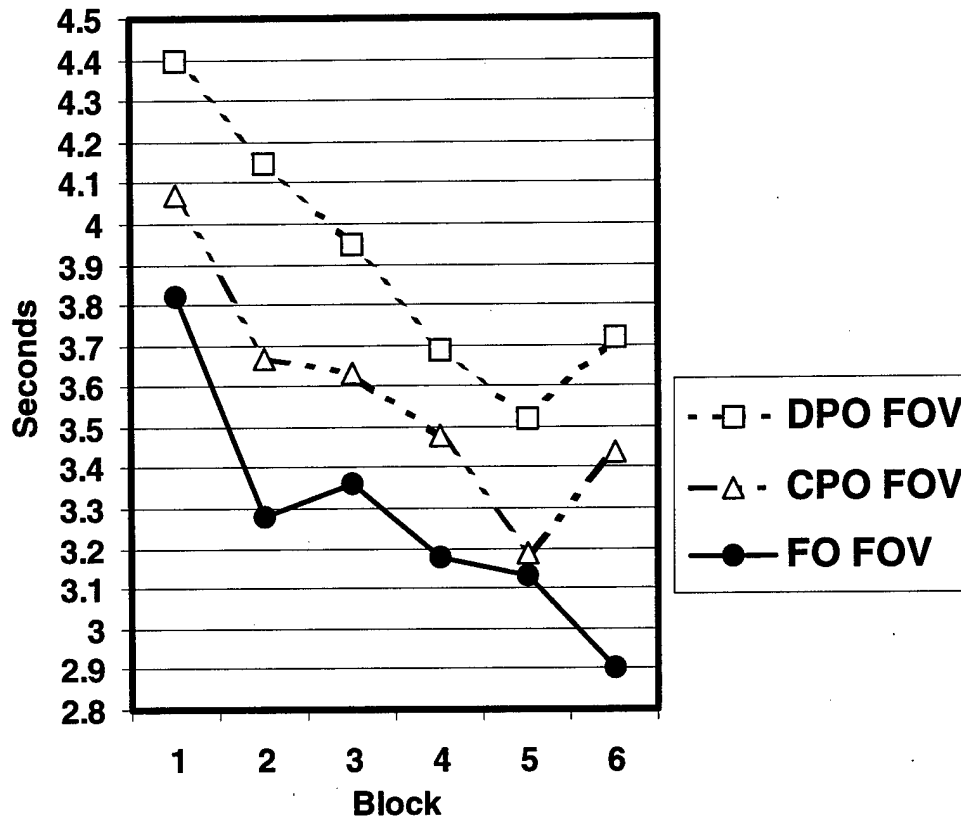


Figure 7. Mean response time to acquire target (FOV x Block).

three FOV configurations are plotted separately. This general improvement in performance continues through the sixth block for the FO FOV and through the fifth block for the CPO and DPO FOVs.

The significant FOV x Position two-way interaction on RT can be seen in Figure 8, where each of the three FOVs, again plotted separately, are not parallel. There was also a significant main effect of FOV on RT, $F(2,28) = 12.48, p = .000133$, as well as a significant main effect of Position on RT, $F(8,112) = 8.97, p < .000001$. The Position main effect per se is not of special interest here as there are many possible confounding factors which can affect RTs to position, such as the preferred scan patterns of observers, or the time to respond with a particular keystroke position. It was not unexpected that the RTs to centrally located and binocular positions would be faster than RTs to lateral and/or monocular targets. Observers in this study were free to use any scan pattern and were not instructed on how to search. While not the focus

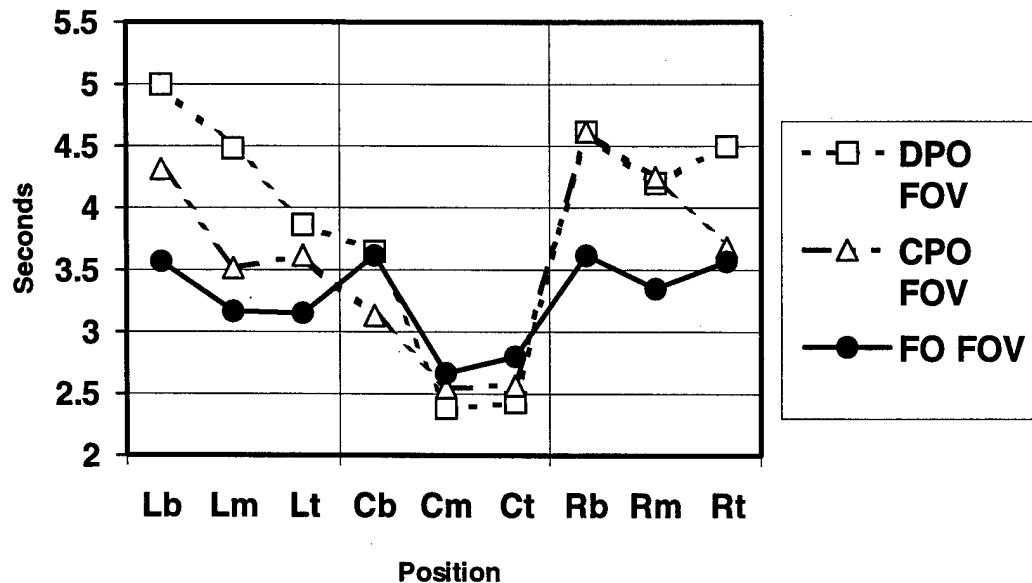


Figure 8. Mean response time to acquire target (FOV x Position).

of our study, it is interesting to note that the bottom positions in each of the three columns of targets have the longest RTs for their respective columns. This would seem to indicate that observers tended to search the top half of the FOV first, although we can not rule out confounding effects of keypad position and so on.

The focus of this study was the effect of FOV configuration on performance. A series of planned comparisons examined the effect of FOV configuration on RT for each of the nine positions. Of these positions, the three center positions, Cb, Cm, and Ct, are binocular under all three FOV configurations, and the lateral positions, Lb, Lm, Lt, Rb, Rm, and Rt, are monocular in the two PO FOVs and binocular in the FO FOV. For each position, our planned comparisons consisted of first, comparing the RTs of the two PO FOVs, the CPO and the DPO, with the RTs of the FO FOV; and second, comparing the RTs of the DPO FOV with the RTs of the CPO FOV.

The mean RTs in seconds (collapsed over blocks) are shown in Table 1, where rows represent the FOVs and columns represent the positions. These are plotted in Figure 8. The means represent the time to respond to the target when the target was in each of the nine positions. The next row gives the results of the planned comparisons testing for a difference between the two PO FOVs and the FO FOV, and the row below it gives the significance level.

Table 1.

Mean response times in seconds, collapsed over blocks, and planned comparisons.

Position	Left			Center			Right		
	bottom	middle	top	bottom	middle	top	bottom	middle	top
DPO FOV	4.99	4.49	3.87	3.66	2.38	2.44	4.61	4.21	4.50
CPO FOV	4.32	3.52	3.61	3.14	2.55	2.57	4.61	4.25	3.68
FO FOV	3.56	3.17	3.16	3.62	2.67	2.80	3.62	3.35	3.56
CPO, DPO FOVs vs FO FOV. F(1,14) =	26.15	363.5	19.34	1.80	0.90	2.17	18.73	18.21	6.31
p =	.0002 **	.0000 **	.0006 **	.201	.359	.162	.0007 **	.0008 **	.025 *
DPO FOV vs CPO FOV. F(1,14) =	3.39	7.48	0.71	3.46	0.55	0.24	0.00006	0.01	5.11
p =	.086	.016 *	.414	.084	.469	.630	.994	.923	.040 *

Note: * = $p < .05$, ** = $p < .01$. Data graphed in Figure 8.

Table 2.

Mean percentage increase in response time, collapsed over blocks.

Position	Left			Center			Right			Row Mean
	bottom	middle	top	bottom	middle	top	bottom	middle	top	
DPO / FO	40	42	23	0.9	- 11	- 13	28	25	26	18
CPO / FO	21	11	15	-13	- 4	- 8	28	27	3	9
DPO / CPO	16	27	7	16	- 7	- 5	-0.7	-1	22	8

With $p < .05$ as our criterion for significance, the results show that there were no significant differences for the three centrally located positions where the targets were binocular in all three FOV configurations. The partial overlapping of the FOV caused a significant increase in RT to locate the target for all the lateral positions where the target was monocular. The target was monocular in the two PO FOVs and binocular in the FO FOV.

How much the CPO and DPO FOVs increased the RT over the FO FOV in percentage terms is shown in Table 2. Partially overlapping the FOV caused the RT to lateral targets to increase an average of from 3 to 42 percent. For all positions, the DPO FOV increased RTs an average of 18 percent, and the CPO FOV increased it an average of 9 percent, but for lateral targets in particular, the average increase was 31 and 18 percent, respectively.

The next to the last row in Table 1 gives the results of the planned comparisons testing for a difference between the CPO FOV and the DPO FOV, and the last row gives the significance levels. With $p < .05$ as our criterion for significance, the results show that there were two significant differences, the Lm and the Rt positions, both lateral positions. The Lb and Cb positions approached significance. In half of the lateral positions, the RT to a target in a DPO FOV was significantly, or close to significantly, longer than to a target in the CPO FOV. The Cb RT were close to significantly longer. How much the DPO FOV increased RT over the CPO FOVs in terms of percentage is shown in the last row of Table 2. Overall, for these lateral positions, the DPO FOV increased RTs an average of 11 percent over the CPO FOV.

As a check on the RT data, the log of each individual RT was used as the input data for statistical analysis. This was to remove the potentially distorting effect that outliers can have on the means in RT data. The following results of the analysis of the logRTs were essentially the same as the analysis of the RTs, with minor differences in significance levels. Again, the three-way Blocks x FOV x Position interaction was not significant, $F(80,1120) = 1.10$, $p = .27$. Again, the two-way Block x FOV interaction was not significant, $F(10,140) = 0.66$, $p = .76$, but this time, the two-way Block x Position interaction marginally reached significance, $F(40,560) = 1.42$, $p = .05$. Again, the two-way FOV x Position interaction was highly significant, $F(16,224) = 5.19$, $p < .000001$. Again, the three main effects were each highly significant: Blocks, $F(5,70) = 7.49$, $p = .000012$; FOV, $F(2,28) = 14.69$, $p = .000043$; and Position, $F(8,112) = 13.80$, $p < .000001$.

Table 3 gives the mean logRTs to locate the target, where the rows and columns in Table 3 correspond to those of Table 1. Below the data rows are the results of the planned comparison testing for a difference between the two PO FOVs and the FO FOV, and below that the significance level. With $p < .05$ as our criterion for significance, the results for the logRTs again show that the partial overlapping of the FOV causes a highly significant increase for all of the lateral positions. In addition, this time, the Cm position marginally reached significance in the reverse direction. The next to the last row gives the results of the planned comparisons testing for a difference between the CPO FOV and the DPO FOV, and the last row gives the significance levels. With $p < .05$ as our criterion for significance, the results again show that identifying the

Table 3.

Mean log of response times (in seconds), collapsed over blocks, and planned comparisons.

Position	Left			Center			Right		
	bottom	middle	top	bottom	middle	top	bottom	middle	top
DPO FOV	0.666	0.600	0.532	0.505	0.277	0.304	0.620	0.570	0.577
CPO FOV	0.583	0.496	0.481	0.441	0.303	0.330	0.613	0.555	0.503
FO FOV	0.522	0.458	0.448	0.498	0.348	0.358	0.533	0.482	0.494
CPO, DPO FOVs vs FO FOV. F(1,14) =	24.22	14.77	31.30	2.54	5.00	2.23	21.95	15.78	5.41
p =	.0002 **	.002 **	.00007 **	.133	.042 *	.157	.0004 **	.001 **	.035 *
DPO FOV vs CPO FOV. F(1,14) =	7.87	10.47	2.21	6.15	0.53	0.50	0.11	0.26	10.05
p =	.014 *	.006 **	.159	.027 *	.477	.489	.743	.621	.007 **

Note: * = $p < .05$, ** = $p < .01$.

target was significantly longer in the DPO than in the CPO for the Rt and Lm positions. Additionally, the Lb and the Cb positions also reached significance. In half of the lateral positions, the mean logRTs to a target in a DPO FOV was significantly longer than to a target in the CPO FOV. The overall results of the analyses examining the logRTs were essentially similar to the results for the raw RTs, with minor differences in significance levels.

Figure 9 graphs the mean number of misses before acquiring the target, collapsed over blocks, and Table 4 lists the means. The numbers are very low, ranging from 0.03 to 0.26, out of a possible range of 0 to 8, which indicates that subjects followed instructions and generally did not guess the target until they were reasonably sure. These data, when subjected to the same 3-way ANOVA as the RT data, show all nonsignificant effects except for a slightly significant main effect of FOV on number of misses, $F(2,28) = 3.62$, $p = .04$. The average was 0.13 for the DPOs, 0.13 for the CPOs and 0.09 for the FOs. This supports the RT data in that there were a higher number of misses for the PO FOVs, which had longer RTs compared to the FO FOV, which had shorter RTs.

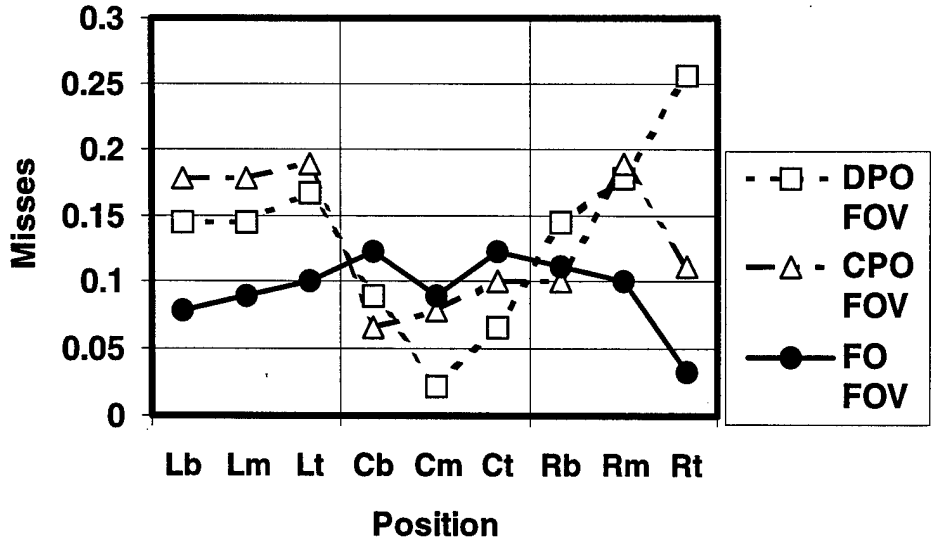


Figure 9. Mean number of misses before target acquisition (FOV x Position).

Table 4.

Mean number of misses (out of a maximum of 8), collapsed over blocks.

Position	Left			Center			Right			FOV Mean
	bottom	middle	top	bottom	middle	top	bottom	middle	top	
DPO FOV	0.14	0.14	0.17	0.08	0.02	0.07	0.14	0.18	0.26	0.13
CPO FOV	0.18	0.18	0.19	0.07	0.08	0.10	0.10	0.19	0.11	0.13
FO FOV	0.08	0.09	0.10	0.12	0.09	0.12	0.11	0.10	0.03	0.09

Note: Data graphed in Figure 9.

Figure 10 graphs the mean percent first scores, the percentage of times the target was acquired on the first guess; that is, the targets that were acquired without misses. Improving performance or increasing percentage increases down the ordinate to bring the graph into conformity with the other graphs. Table 5 lists the mean percent first scores (collapsed over

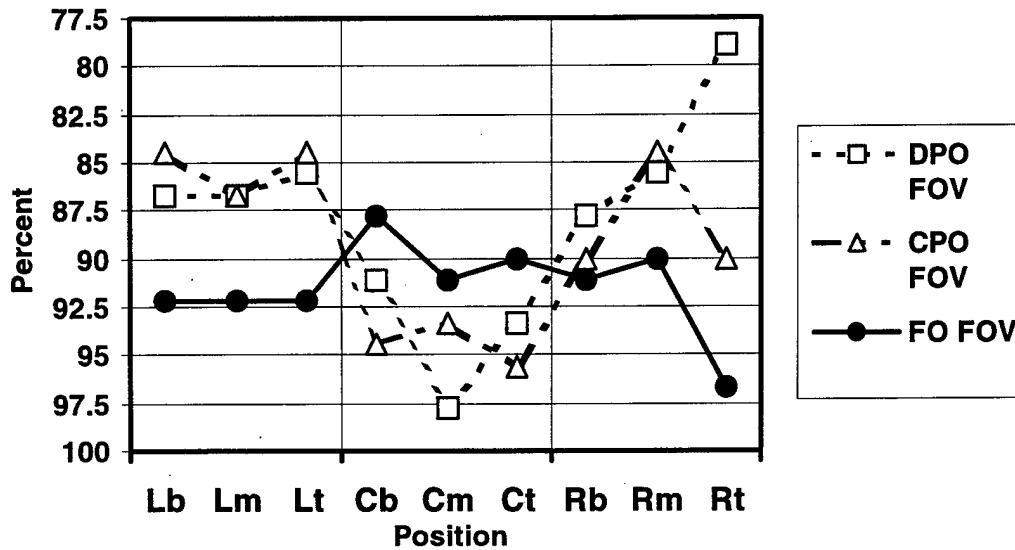


Figure 10. Mean percent of first scores (FOV x Position).

Table 5.
Mean percent of first scores, collapsed over blocks.

Position	Left			Center			Right			FOV Mean
	bottom	middle	top	bottom	middle	top	bottom	middle	top	
DPO FOV	87	87	86	91	98	93	88	86	79	88
CPO FOV	84	87	84	94	93	96	90	84	90	89
FO FOV	92	92	92	88	91	90	91	90	97	91

Note: Data graphed in Figure 10.

blocks). These data when subjected to the same 3-way ANOVA as the RT data showed all non-significant effects except for a marginally significant main effect of FOV on percent first scores, $F(2,28) = 3.35$, $p = .05$. The average was 88.3 for the DPOs, 89.1 percent for the CPOs, and 91.4

percent for the FOs. There were lower percent first scores for conditions that had longer RTs and for conditions that had a higher number of misses.

The mean number of misses are relatively small compared to a possible maximum of eight, with four the chance response; and the mean percent first scores are within three percentage points of each other, which indicates there is unlikely to be any speed accuracy tradeoff in these data. A speed accuracy tradeoff would be suspected if the conditions with the faster RTs had lower accuracies, and the conditions with the slower RTs had higher accuracies. If there had been large differences in the number of misses, and large percent first score differences in the opposite direction to the RT data (i.e., relative performance was better by one measure and poorer by another), then there would have been a concern with the interpretation of the data because of the need to determine the function of the speed accuracy tradeoff. However, the number of misses and percent first scores data are in the same direction as the RT data, and so, if anything confirm, rather than mitigate the conclusions one draws from the RT data concerning which are the easier or harder conditions in terms of overall performance. Compare the similar patterns of Figures 9 and 10 with Figure 8. It is interesting to note that, for the center positions, performance with the CPO and DPO FOVs is slightly better, though not significantly better, than in the FO FOV. It is possible that in the PO conditions, the center region tends to draw the observer's attention to the detriment of the lateral regions, while in the FO FOV, the subject tends to more evenly spread attention over the entire FOV. Though this cannot be determined from these data, the slight performance improvements for the POs over the FO to targets in the central region of the FOV may be due in large part to the smaller relative area of the binocular portion of the FOV where subjects tend to focus attention.

In summary, on average, performance was best in the FO FOV, where RTs were fastest, and worst in the DPO FOV, where RTs were slowest. These performance differences tended to be confirmed by the number of misses and the percent first score data. The differences between FOV configurations tended to be most pronounced for lateral targets, which were in monocular regions in the PO FOVs.

Conclusions

Moffitt (1989) suggested that the contours that occur in an FOV displaying a natural scene should eliminate the luning, and presumably, the other detrimental effects such as reduced visibility of targets that occur in partial binocular overlap displays. One might assume that the added contours would bias the binocular rivalry to the monocular image that contains the contours, the real world scene and the targets, as opposed to the opposing image which only contains a black background and one contour, the binocular border. Our displays were highly cluttered with background contours from the randomly placed ellipses, and yet, the RT results reflect the results found in the previous luning, fragmentation, and target visibility studies: Performance is highly significantly affected by PO FOVs, more so in the DPO FOV than in the CPO FOV. This was true even though our targets were well above threshold for most of their

flicker cycle. Also, any stimulus that moves or flickers is known to bias binocular rivalry to the benefit of the moving or flickering target (Arditi, 1986; Fox, 1991; Fox and Check, 1968, 1972), but the added clutter contours and flickering suprathreshold targets did not remove the detrimental effects on performance of partially overlapping the FOV.

There is a tradeoff in enlarging the FOV by the partial overlap method. The FOV is larger, but as this study shows, PO can have significant human performance consequences. In our experiment, average time to find a target increased by as much as 31 percent for divergent and 18 percent for convergent FOVs. This preliminary study found that performance decrements due to FOV configurations parallel the previously found psychophysical decrements. The relative contributions of different factors to the performance decrements with PO configurations and possible ways to alleviate it need to be further investigated.

References

- Alam, M. S., Zheng, S. H., Iftekharruddin, K. M., and Karim, M. A. 1992. Study of field-of-view overlap for night vision applications. Proceeding of the 1992 IEEE National Aerospace and Electronics Conference, NEACON Vol 3, 1249-1255. Dayton, OH.
- Arditi, A. 1986. Binocular vision. In (K. R. Boff, L. Kaufman, and J. P. Thomas) Handbook of perception and human performance, Vol. 1. New York: John Wiley & Sons.
- Edgar, G. K., Carr, K. T., Williams, M., and Clark, A. L. 1991. The effect upon visual performance of varying binocular overlap. AGARD symposium on helmet-mounted displays and night vision goggles, Neuilly-sur-Seine, France. (AGARD Conference Proceedings 517), 8-1 to 8-15.
- Fox, R. 1991. Binocular Rivalry. In (D. Regan), Vision and visual dysfunction, Vol. 9., 93-110.
- Fox, R., and Check, R. 1968. Detection of motion during binocular rivalry suppression. Journal of experimental psychology, 78(3), 388-395.
- Fox, R., and Check, R. 1972. Independence between binocular rivalry suppression duration and magnitude of suppression. Journal of experimental psychology, 93(2), 283-289.
- Kaufman, L. 1963. On the spread of suppression and binocular rivalry. Vision research, 3, 401-415.
- Kaufman, L. 1964. Suppression and fusion in viewing complex stereograms. American journal of psychology, 77, 193-205.
- Kenyon, R. V., and Kneller, E. W. 1993. The effects of field of view size on the control of roll motion. IEEE transactions on systems, man, and cybernetics, 23(1), 183-193.
- Klymenko, V., Verona, R. W., Beasley, H. H., Martin, J. S., and McLean W. E. 1994a. Factors affecting fragmentation of partial binocular overlap displays. Fort Rucker, AL: U.S. Army Aeromedical Research Laboratory. USAARL Report 94-29.
- Klymenko, V., Verona, R. W., Martin, J. S., Beasley, H. H., and McLean W. E. 1994b. Factors affecting the perception of luning in monocular regions of partial binocular overlap displays. Fort Rucker, AL: U.S. Army Aeromedical Research Laboratory. USAARL Report 94-47.
- Klymenko, V., Verona, R. W., Martin, J. S., Beasley, H. H., and McLean W. E. 1994c. The effect of binocular overlap mode on contrast thresholds across the field-of-view as a function of spatial and temporal frequency. Fort Rucker, AL: U.S. Army Aeromedical Research Laboratory. USAARL Report 94-49.

- Kruk, R., and Longridge, T. M. 1984. Binocular overlap in a fiber optic helmet mounted display. The image 3 conference proceedings, 363, 363-377. Brooks Air Force Base, TX: Air Force Human Resources Laboratory, Air Force Systems Command. AFHRL-TR-84-36.
- Landau, F. 1990. The effect on visual recognition performance of misregistration and overlap for a biocular helmet mounted display. SPIE proceedings, Vol. 1290, helmet-mounted displays II, 173-184. San Jose, CA: SPIE-The International Society for Optical Engineering.
- Melzer, J. E., and Moffitt, K. 1989. Partial binocular overlap in helmet-mounted displays. SPIE Proceedings, Vol. 1117, display system optics II, 56-62. San Jose, CA: SPIE-The International Society for Optical Engineering.
- Melzer, J. E., and Moffitt, K. 1991. An ecological approach to partial binocular-overlap. SPIE proceedings, Vol. 1456, large screen projection, ionic, and helmet-mounted displays, 175-191. San Jose, CA: SPIE-The International Society for Optical Engineering.
- Moffitt, K. 1989. Luning and target detection. San Jose, CA: Kaiser Electronics.
- Moffitt, K. 1991. Partial binocular overlap: concepts, research, & systems. San Jose, CA: Kaiser Electronics.
- Moffitt, K., and Melzer, J. 1991. Partial binocular overlap. San Jose, CA: Kaiser Electronics.
- Osgood, R. K., and Wells, M. J. 1991. The effect of field-of-view size on performance of a simulated air-to-ground night attack. AGARD symposium on helmet-mounted displays and night vision goggles (AGARD Conference Proceedings 517), 10-1 to 10-7., Aerospace medical panel symposium, Pensacola, FL.
- Wells, M. J., Venturino, M., and Osgood, R. K. 1989. The effect of field-of-view on performance at a simple simulated air-to-air mission. SPIE proceedings, Vol. 1116, helmet-mounted displays, 126-137. San Jose, CA: SPIE-The International Society for Optical Engineering.
- Wolpert, L. 1990. Field-of-view information for self-motion perception. In (R. Warren and A. H. Wertheim) Perception and control of self-motion. Hillsdale, NJ: Lawrence Earlbaum Associates.

Appendix

List of manufacturers.

Hewlett-Packard Co.
3404 East Harmony Road.
Fort Collins, CO 80525